Protective Role of Akt1 in Amyloid Beta Peptide Induced Degeneration in Alzheimer's Disease

Thesis submitted in partial fulfillment of the requirements of
Five Year BS-MS Dual Degree Program

Indian Institute of Science Education and Research, Pune

By

Prarabdha Jagdhane

At

Centre for Neuroscience

Indian Institute of Science, Bangalore

Project Guide

Prof. Vijayalakshmi Ravindranath

Centre for Neuroscience,

Indian Institute of Science,

Bangalore

Project Advisor,

Dr. Aurnab Ghose

Indian Institute of Science

Education and Research,

Pune

Certificate

This is to certify that this dissertation entitled "Protective Role of Akt1 in Amyloid Beta Peptide Induced Degeneration in Alzheimer's Disease" towards the partial fulfillment of the BS-MS dual degree programme at the Indian Institute of Science Education and Research, Pune represents original research carried out by "Prarabdha Jagdhane at Indian Institute of Science, Bangalore" under the supervision of "Prof. Vijayalakshmi Ravindranath, Chairperson, Centre for Neuroscience" during the academic year 2014-2015.

Prof. Vijayalakshmi Ravindranath
Chairperson,
Centre for Neuroscience,
Indian Institute of Science, Bangalore

The Chairperson
Centre for Neuroscience
Indian Institute of Science
Bangalore - 560 012

Declaration

I hereby declare that the matter embodied in the report entitled “Protective Role of Akt1 in Amyloid Beta Peptide Induced Degeneration in Alzheimer’s Disease” are the results of the investigations carried out by me at the Centre for Neuroscience, Indian Institute of Science, Bangalore, under the supervision of Prof. Vijayalakshmi Ravindranath and the same has not been submitted elsewhere for any other degree.

Date: 24th March, 2015

Prarabdha Jagdhane
B.S-M.S Dual Degree Student
Indian Institute of Science Education and Research, Pune

Abstract

Alzheimer's disease (AD) is one of the most common neurodegenerative disorders in elderly, characterized by loss of higher cognitive functions. The major hallmarks of AD seen in late stages are gross neurodegeneration, presence of extracellular amyloid plaques and intracellular neurofibrillary tangles. But in the recent years, there has been paradigm shift in AD research. It is now clear that synapse is the main target of attack in AD, with spine and synapse loss thought to be an early event in AD pathologies. Research in our lab has shown that oxidative stress could potentially play a critical role in mediating synaptic dysfunction through redox modifications of key proteins at the synapse leading to signaling changes. Studies in our laboratory have showed a critical role of Protein Kinase B (PKB, also called Akt1); a protein implicated in cell survival pathways, in activity-dependent translation. Moreover, we have also observed a synapse-specific deregulation of Akt1 signaling very early in our AD mouse model, indicative of its role in the pathogenesis of AD. Hence, deregulation of Akt1 signaling and consequent disrupted activity-dependent synaptic protein translation might culminate into compromised synaptic function and plasticity, activation of molecular cell death pathway and or reduction of cell survival signaling. Deregulation of Akt1 signaling in AD mouse model indicates that it might play a crucial role in synaptic dysfunction/ spine loss observed in AD. Hence, the objective of this study is to assess if Akt1 overexpression can be used as a protective measure to rescue synaptic function in AD. To this end, a lentiviral construct expressing myristoylated Akt1 (MyrAkt1) fluorescently tagged with pmCherry marker is produced with a titer value of 2.2×10^6 TU/ml. And its effect on spine pathology will be monitored upon over-expressing it in primary cortical culture derived from APP/PS1 transgenic mice.

Table of Content

List of figures

Acknowledgements

Working on this project was an exciting and intellectually enriching experience. I would like to thank Indian Institute of Science for giving me an opportunity to carry out my Master of Science thesis project. I am highly indebted to my guide, Prof. Vijayalakshmi Ravindranath, centre for neuroscience, Indian Institute of Science, Bangalore for permitting me to avail her lab facilities for the project work. I thank her for her encouraging guidance and providing me with great scientific atmosphere. Apart from research, I have learnt a lot on how and why to pursue research. These molded my overall scientific development for which I am heavily indebted to her.

I am highly grateful to my advisor Dr. Aurnab Ghose, Indian Institute of Science Education and Research, Pune for his valuable, inspiring and timely advice during my project work.

I owe particular thanks to Dr. Balaji Jayaprakash, Aditi Verma, Khader Valli, Eisha Shaw, Debajyoti Das, for teaching and guiding me through various techniques with encouragement and enthusiasm. I thank them for the moral support and all kinds of help they offered to make my stay comfortable.

I am thankful to all my lab members Ajit Ray, Faraz Ahmad, Arathy Ramachandran, Ruturaj Gowaikar, Reddy, Bodhisatwa Chaudhuri, Sunny Kumar, Arunabha Chakrabarti, Kamalika Chakrabarti, Meghashree, and Disha for encouraging me all through the project and for maintaining a fun atmosphere in the lab.

Special thanks are owed to my parents, who have supported me throughout my years of education, both morally and financially.

I thank IISER Pune for providing me this wonderful opportunity to grow and develop both scientifically and personally.

1. Introduction

1.1 Historical Perspective

Alzheimer's disease (AD) is one of the most common neurodegenerative disorders in the elderly, characterized by loss of memory and cognitive impairment. It is a debilitating progressive neurodegenerative disease, affecting over 27 million people worldwide. AD was first described by a German psychiatrist and neuropathologist Alois Alzheimer in 1906 and was named after him. The disease progresses gradually, in an age dependent manner and results in loss of memory, personality changes and decline in cognitive functions. Neuropathologically, AD is characterized by: 1) neurodegeneration in areas of the brain responsible for memory formation and cognition, 2) the presence of aggregated forms of proteins in the extracellular spaces, referred to as amyloid plaques, throughout the brain and 3) intracellular protein deposits termed as neurofibrillary tangles (Arendt, 2009). Neurofibrillary tangles are deposits of hyperphosphorylated protein, tau. Amyloid plaques are deposits of aggregated proteins in the extracellular space of the brain (Braak and Braak, 1991). There are two forms of the disease: an early onset familial form that follows Mendelian laws of inheritance and the late onset heterogeneous form that shows no discernable mode of inheritance at a single loci, hence also called sporadic AD. Most cases of early onset AD are caused by mutations in genes encoding Amyloid Precursor Protein (APP), Presenilin1 (PS1) and Presenilin2 (PS2), the proteins that form the catalytic part of the γ-secretase complex that cleaves APP to give Aβ42 peptide (Bertram and Tanzi, 2008). All these mutations show autosomal dominant inheritance and lead to increased production of Aβ42 (William et al., 2012). On other hand, late onset, sporadic AD accounts for 90% of the cases. No specific gene mutations associated with the disease are known. However, genome wide association studies have uncovered susceptibility genes including apoliproteinE4 (apoE), neprilysin, insulin degrading enzyme and alpha 2 macroglobulin that lead to increased risk of the disease (Bertram and Tanzi, 2011).

In the recent years, there has been paradigm shift in AD research with AD now being considered as primarily a synaptic disorder. A striking discovery that further opened new vistas in AD research was the finding that synapse loss strongly correlated with both

soluble Aβ42 levels as well as decline of cognitive functions (Cleary et al., 2005; Scheff et al., 2006). In the earliest stages of AD, the disease manifests as a pure impairment of cognitive functions beginning as an inability to form new memories, first of trivial and then gradually of important life events. The symptoms present in such an insidious fashion so as to be commonly mistaken as either age-related or stress-related problems. These impairments occur in the absence of any overt cell damage or loss, in individuals whose motor and sensory functions are preserved and neurologically intact. As the disease progresses, both declarative and non-declarative memory functions decline with eventual loss of the power of reasoning and abstracting and finally language. But it is the earliest manifestation of the disease which indicates that the disease initiates at the synapses, which are now known to be the cellular correlate of memory (Townsend et al., 2006). So if we are to elucidate and understand the pathogenesis and progression of AD, we have to look at the covert presymptomatic changes that take place at the synapses in the brain areas responsible for memory and cognition, much before pathological symptoms of neurodegeneration are seen. Studies have already shown that in mice models of AD, expressing mutated forms of APP, there is loss of pre-synaptic terminals as the levels of soluble Aβ42 rises (Tu et al., 2014). Furthermore; electrophysiological recordings have shown deficits in basal transmission and impaired long term potentiation in the hippocampus much before the appearance of Aβ deposits (Srivareerat et al., 2009). It is interesting to note that none of the known animal models of AD, expressing mutated APP, show any neurodegeneration measured as cell loss. These animals show the gamut of behavioral deficits expected in an AD model and amyloid plaques. This again indicates that cell death is a relatively advanced feature in the disease and causational events start working much before cell death initiates.

1.2 Pathological mechanisms of synaptic dysfunction

The challenge now is to elucidate the mechanism by which Aβ42 triggers changes in the synapses leading to dysfunction and loss. Of the many possible mechanisms implicated in synapse dysfunction in AD, oxidative stress plays an important role in mediating synapse dysfunction early in the disease process before overt Aβ42

aggregation has occurred and behavioral symptoms emerge (Varadarajan et al., 1999). Another possible mechanism may involve Aβ42 oligomers acting as ligands for receptors such as RAGE and PSD95 which transduce signal inside the cell, initiating signaling cascades leading to changes at the synapse (Proctor et al., 2010).

Redox modification is now recognized as an important post-translational modification in signaling. Major perturbation in the redox homoeostasis of the cell would cause the proteins to be irreversibly changed in structure and function (Sultana and Butterfield, 2009). Research from our lab has shown that two critical proteins actin and Akt play important roles at the synapse. Actin is a major cytoskeleton protein at the synapses being highly enriched at dendritic spines, the post synaptic compartments that mediate most of the excitatory synaptic transmission in the brain (Hering and Sheng, 2001). On the other hand, Akt is an important kinase known to play a key role in regulation of protein translation via modulation of protein translation machinery proteins 4EBP1 and S6K (Griffin et al., 2005). It is observed that myriad physiological processes such as synapse development, function and plasticity are the result of changes occurring in the structure and number of dendritic spines (Penzes and Jones, 2008). Synapses are the sites where AD pathogenesis likely initiates and signaling pathways have been found to be highly concentrated in the synaptic terminals (DeKosky and Scheff, 1990; Scheff and Price, 2003). Thus abnormal signaling in synaptic terminals would be suspected to play a major role in pathogenesis of this disorder.

1.3 Role of Protein Kinase B (PKB)/Akt at synapse and AD

Protein kinase B (PKB), also known as Akt, is a serine/threonine-specific protein kinase which has three highly homologous members known as Akt1, Akt2 and Akt3 in mammalian cells. It plays an important role in the transmission of signals from growth factor receptors to regulate gene expression and function as a critical regulator of protein translation, cell survival, proliferation and nutrient metabolism among others. Akt consists of conserved domain structure, comprising a specific pleckstrin homology (PH) domain, a central kinase domain and a carboxyl-terminal regulatory domain that mediates the interaction between signaling molecules (Song et al., 2005). Myristoylation

of PKB/Akt promotes constitutive membrane attachment and activation causing an increase in its basal level of phosphorylation (Kohn et al., 1996).

Akt is known as critical survival protein in the cells. At the synapse, however, Akt is implicated in a variety of signaling primarily involved in local protein translation. Research from our lab now has shown a significant loss of Akt signaling specifically at the synapse at an early age in Transgenic mice [B6C3-Tg (APPswe, PSEN1)85Dbo/J] (APP/PS1). Further, it is observed that this loss translates into a loss of signaling of downstream targets, pmTOR and pS6K/p4EBP1 (Ahmad et al., unpublished data). The pmTOR pathway is involved in activity dependent protein translation at the synapse (Datta et al., 1999; Scheid and Woodgett, 2000). Loss of this critical signaling in APP/PS1 mice indicates that activity dependent protein translation could be compromised very early on, in these animals leading to far reaching implications in AD pathogenesis. Recently it is been observed that Akt1 is a critical mediator of growth factor induced neuronal survival which can suppress apoptosis (Song et al., 2005). Different components of the apoptotic machinery are phosphorylated and in-turn inactivated by activation the serine/threonine kinase Akt1. Thus induced Akt activity due to overexpression might be sufficient to block apoptosis and spine loss.

1.4 Lentivirus vector

In recent years, Lentivirus has become one of the most widely used vectors for gene therapeutic applications. Lentivirus belongs to a genus of slow virus with long term, stable transgenic expression and has an ability to induce a wide range of pathologies in different animal species (Breckpot et al., 2003). Characteristic features of lentiviruses are: 1) Stable incorporation into target cells. 2) Absence of contaminating viral proteins. 3) Absence of replication competent virus and tendency to efficiently target non-dividing and differentiated cells, such as neurons or dendritic cells (Bukrinsky et al., 1993). As such, these vectors are broadly used in a multitude of in vivo and ex vivo gene therapy applications (Lewis and Emerman, 1994).

Lentivirus life cycle starts with the binding of the viral envelope to its receptor, further the particle is uncoated and the core is released into the cytoplasm. Within the core

single strand RNA (ssRNA) is reverse transcribed into double stranded DNA (dsDNA) which then gets transported to the nucleus (Bukrinsky et al., 1993). The viral DNA gets integrated into the host DNA which then gets translated resulting in long-term expression of viral genes, leading to maturation of virions which results into budding of the particle from the cell, giving infectious virions (Palù et al., 2000).

Lentiviral vectors are produced in a transient transfection system in which a cell line is transfected with three separate plasmid systems. These include the transfer vector plasmid, packaging plasmid and envelope plasmid (Mautino, 2002). The transfer vector plasmid contains cis-acting genetic sequences necessary for the vector to infect the target cell and for transfer of the reporter gene. It contains restriction sites for insertion of desired genes (Naldini et al., 1996). The packaging plasmid contains elements required for vector packaging such as structural proteins and the enzymes that generate vector particles (Mautino, 2002). The envelope plasmid consists of two types of heterologous envelope proteins, the amphoteric envelop of MLV and G glycoproteins of the vesicular stomatitis virus, known as VSV-G. Both of these help to provide stability to the vector by bringing together the particles that were made by the packaging plasmid (Naldini et al., 1996).

Based on the packaging plasmid lentiviral particles are divided into different generations. The first generation packaging plasmid comprises of gag and pol sequences; vif, vpr, vpu and nef accessory genes and tat, rev viral regulatory genes. In second generation plasmid the lentivector safety is improved by removing four accessory genes, vif, vpr, vpu and nef without affecting the vector yield or infection efficiency (Zufferey et al., 1997). Third generation packaging systems consists of a split-genome packaging system which further improves the lentivector safety. In third generation packaging system the rev gene is expressed from a separate plasmid and the 5′LTR from the transfer vector replaced by a strong tat-independent constitutive promoter (Dull et al., 1998).

2. Rationale and Hypothesis

Genetic, biochemical and behavioral research from both familial and sporadic forms of the disease suggest that enhanced accumulation, either due to overproduction or decreased degradation of the neurotoxic Aβ peptide; from sequential amyloid precursor protein (APP) proteolysis is the crucial step in the development of AD (Bertram and Tanzi, 2008). Another cardinal feature observed in early stage of AD is synaptic dysfunction and loss of dendritic spines. Various mechanisms have been proposed for this dysfunction including deregulation of protein turn-over (Mondragón-Rodríguez et al., 2013). Protein translation, especially activity-dependent protein translation, is critical for synaptic function and relay of neurotransmitter signal in the post-synapse (Komatsuzaki et al., 2012). Our laboratory has now demonstrated that activity-dependent protein translation is negatively affected in a double transgenic mouse model of AD. Interestingly, studies in our laboratory have also showed a critical role of Protein Kinase B (PKB, also called Akt1); a protein implicated in cell survival pathways, inactivity-dependent translation using pharmacological inhibition studies (Ahmad et al., unpublished data). This is not surprising since Akt1-mTOR signaling is known to play a key role in regulation of protein translation via modulation of protein translation machinery proteins 4EBP1 and S6K (Griffin et al., 2005). Moreover, we have also observed a synapse-specific deregulation of Akt1 signaling very early in our AD mouse model, indicative of its role in the pathogenesis of AD. Hence, deregulation of Akt1 signaling and consequent disrupted activity-dependent synaptic protein translation might culminate into activation of molecular cell death pathway and/or reduction of cell survival signaling.

2.1 Specific aims

Deregulation of Akt1 signaling in AD mouse model indicates that it might play a crucial role in synaptic dysfunction and spine loss observed in AD. Hence, the objective of this study is to demonstrate the protective role of Akt1 in AD.

1) To this end, transfer vector plasmid will be cloned consisting of plentiCamKII (backbone), myristoylated Akt1 (MyrAkt1) (gene of interest) and pmCherry (fluorescent tag).
2) Further, viral tool having a lentiviral construct expressing myristoylated Akt1 (MyrAkt1) fluorescently tagged with pmCherry marker will be generated.
3) Later, primary cortical cultures derived from APP/PS1 transgenic mice will be obtained and with the help of immunohistochemical techniques, the effect of over-expression of MyrAkt1 on spine pathology will be investigated.

3. METHODOLOGY

3.1 Animals

Transgenic mice [B6C3-Tg (APPswe, PSEN1)85Dbo/J] were bred in the animal facility at Indian Institute of Science. All animal experiments were carried out as per the institutional guidelines for the use and care of animals.

3.2 Cell Lines and Culture

HEK293T and HEK293FT cells were used to produce lentivirus and Neuro2A and primary cortical cells were used to carry out the experiment. The HEK293T and HEK 293FT cells were grown in DMEM media supplemented with 10% FBS whereas Neuro2A were grown in EMEM media supplemented with 10% FBS.

3.3 Plasmids

The plasmids used in the study were plentiCamKII empty vector, PsPAX2 (packaging plasmid), pMD2.G (envelop plasmid). The plasmids were grown up using Qiagen mini and midi-prep kits.

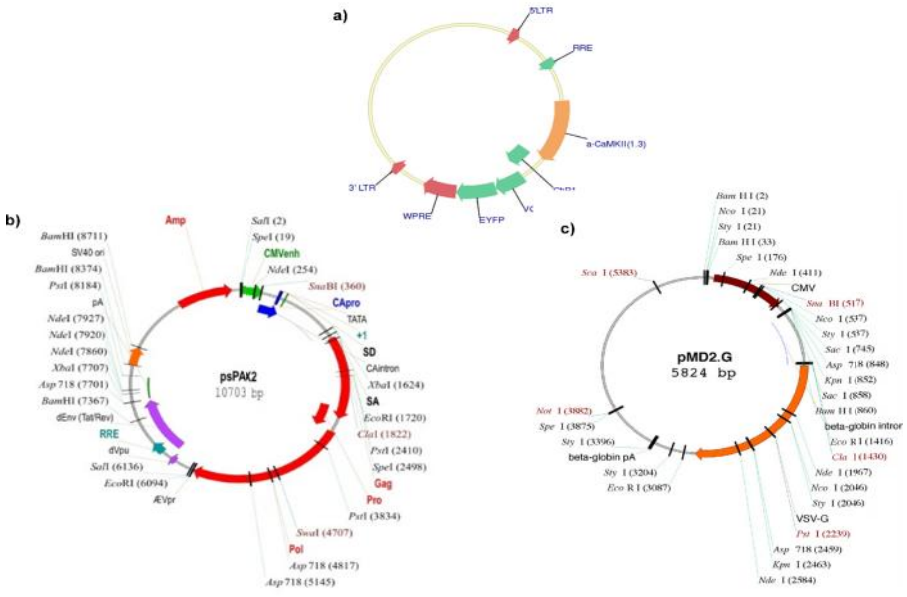

Fig 1: Map of Plasmid used to generate lentivirus a) plentiCamKII plasmid; b) psPAX2 (packaging plasmid) and c) pMD2.G (envelop plasmid) (www.addgene.org)

3.4 PCR based Cloning

Gene specific primers were designed for PCR based cloning.

1) For MyrAkt1
    - Forward primer with BamHI site
      ATAAGGATCCGCCACCATGGGGAGCAGCAAGAGCAAG
    - Reverse primer with KpnI site
      CATAAGGTACCGCAATAGGCTGTGCCACTGGCTGAGTA
2) For pmCherry
    - Forward primer with KpnI
      ATACAGGTACCATGGTGAGCAAGGGCGAGGA
    - Reverse primer with EcoRI
      CTCTAGAATTCTCATTACTTGTACAGCTCGTCCATGCCG

PCR amplicons were identified and isolated using gel electrophoresis followed by gel elution. plentiCamKII plasmid was digested using EcoRI and BamHI restriction enzyme. plentiCamKII backbone (vector), MyrAkt1 (insert) and pmCherry (fluorescent tag) was isolated using gel purification. MyrAkt1and pmCherry templates were obtained from addgene plasmid 49186: pBSFI-myr-akt1 and PT3975-5: pmCherry-C1 respectively. The MyrAkt1 and pmCherry was ligated at KpnI restriction sites. Then MyrAkt1-pmCherry ligated construct was inserted into plentiCamKII backbone. Further, transformation of the ligated reaction into competent cells *E.coli* DH5α was carried out. Plasmid was then isolated and verified using restriction digestion and sequencing. Expression of MyrAkt1 was confirmed using western blot.

For negative control, plentiCamKII plasmid was digested using EcoRI and BamHI restriction enzyme. plentiCamKII backbone (vector), pmCherry (fluorescent tag) was isolated using gel purification. pmCherry was ligated into plentiCamKII backbone. Transformation of the ligated reaction into competent cells *E.coli* DH5α was carried out. Plasmid was then isolated and verified using restriction digestion and sequencing.

For lentivirus generation, packaging plasmid (PsPAX2) and envelop plasmid (pMD2.G) were obtained from Dr. Balaji Jayaprakash's lab as glycerol stubs of transformed

bacteria. These bacteria were grown in ~500 ml of culture using LB broth with ampicillin. Plasmid was extracted using alkaline lyses method.

Transfer vector plasmid (MyrAkt1-pmCherry construct), negative control plasmid, packaging plasmid and envelop plasmid were then amplified and purified using Qiagen midi-preparation.

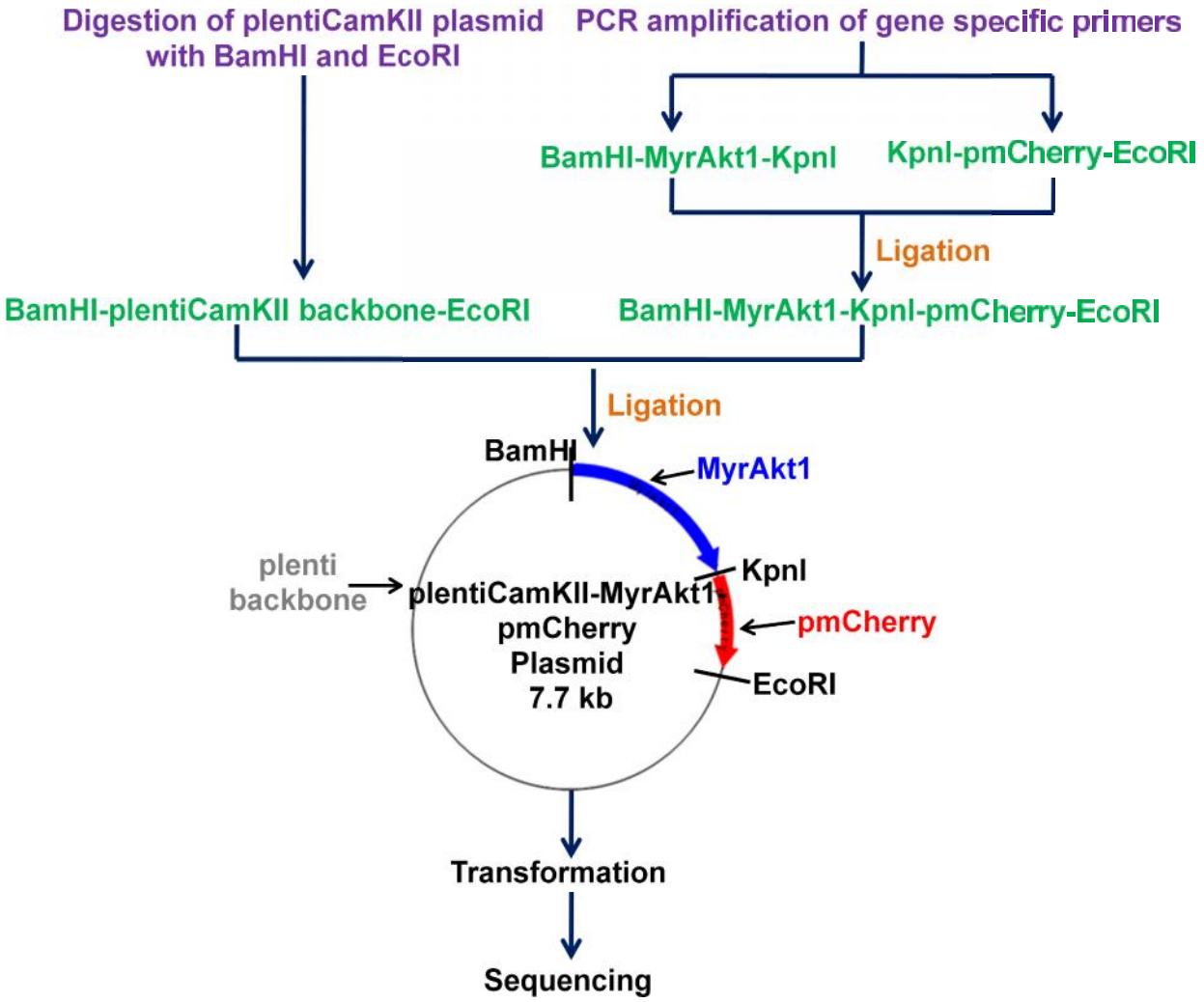

Fig 2: Cloning strategy to clone transfer vector plasmid (plentiCamKII-MyrAkt1-pmCherry)

3.5 Establishment of Cell Culture and Virus Production

HEK293FT culture was standardized for large scale culture of cells for virus generation and purification. Protocol for calcium phosphate mediated transfection of HEK293FT cells was standardized. Second generation lentiviral packaging system was used to generate lentivirus.

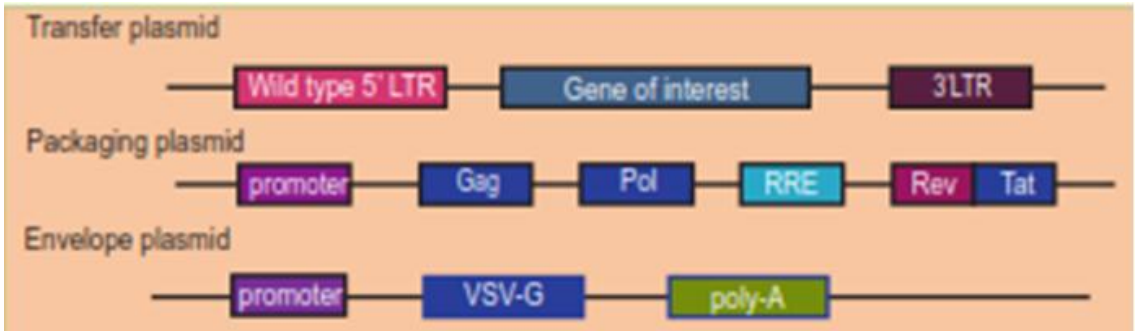

Fig 3: Schematic drawing of 2nd generation lentivirus packaging system (www.cyagen.com/lentivirus-handling-biosafety-consideration-guidlines)

3.5.1 Virus Preparation

HEK293FT cells were cultured in D10 medium (DMEM + 10% FBS + 1% Sodium Pyruvate + 1% Geneticin). Sodium pyruvate is added as an additional source of energy and has protective effects against hydrogen peroxide. 24 hours after plating the cells, they were transfected using calcium phosphate method (calcium phosphate method was obtained from Optogenetics protocol website, http://web.standard.edu/group/dlab/ optogenetics/expression systems.html). In a 100 mm plate (~90% confluent) 15 µg of MyrAkt1-pmCherry plasmid, 15 µg of psPAX2 plasmid and 9.8 µg of pMD2.G plasmid were added. All three plasmids were mixed with calibrated volumes of 2 M calcium chloride, distilled water and 2x HBS buffer. This mixture was further mixed with D10 medium and added to cells. After 16 hours of adding transfection mix, cells were washed with D10 medium and after 24 hours virus production media was added, comprised of serum free medium (Lonza) and sodium butyrate.

3.5.2 Virus Purification and concentration

About ~48 hours after transfection, virus medium was collected from all the culture dishes without disturbing the cells to avoid interference from cell debris during virus concentration. Cell debris were pelleted by centrifugation and filtered through 0.45-mm PVDF membrane filters. Higher titer stocks were obtained by ultra-filtration (Millipore) using density gradient centrifugation at 25,000 rpm for 2:45 hours at 4°C. Virus concentrate was stored in 10 µl aliquots at -80^{o} C.

3.5.3 Virus Titer

Lentiviral titers were determined by seeding HEK293T cells in 12-well plates at 50,000 cells per well the day before infection. 24 hours later, increasing volume of concentrated virus stock ranging from 10-30 µl was added with polybrene (Hexadimethrine bromide) (5mg/ml) to each well. After 36 hours incubation, the culture medium was changed and the cells were incubated for 3 days. Cells expressing pmCherry were identified using fluorescence microscopy. Titers ranged from 1.8 to 2.4×10^{6} infectious units (IU/ml).

Using 30 µl viral concentrate, ~66% transduction efficiency was achieved in ~100% confluent well. Estimated number of cells in each well was ~1×10^{5}

$$\text{Number of cells infected per 30 µl viral concentrate} = \frac{66 \times 1 \times 10^{5}}{100} = 6.6 \times 10^{4} \text{ cells}$$

=> Cells infected per µl = 2.2 × 10^{3} cells (Number of infectious units per micro-liter)
=> We have approximately 2.2 × 10^{6} infectious units per milliliter of concentrate.

$$\text{Multiplicity of Infection (MOI)} = \frac{0.500 \times 2.2 \times 10^{6}}{1 \times 10^{5}}$$

$$= 11$$

Calculation

1) Titer value (transfection unit (TU)/ml) = $\frac{\text{Seeded cells} \times \% \text{ infection} \times \text{dilution factor}}{\text{Volume added in ml}}$

2) Multiplicity of infection (MOI) = $\frac{\text{Volume of virus (ml)} \times \text{titer (ml)}}{\text{Number of cells}}$

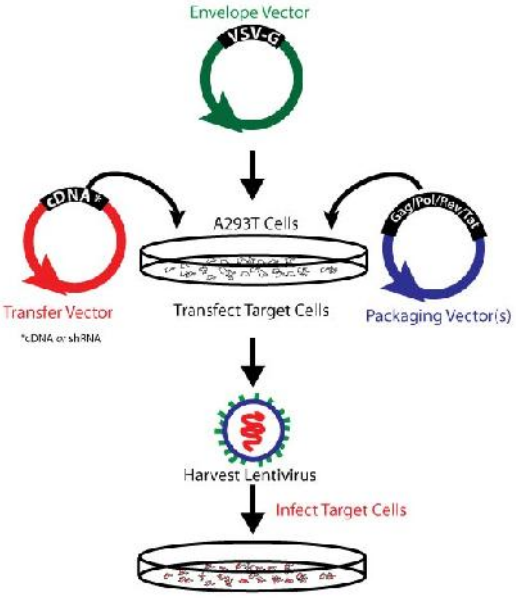

Fig 4: Lentivirus Production
(https://www.addgene.org/lentiviral)

3.6 Western blot

Cells were lysed in PBS by probe sonicator. The homogenate was centrifuged at 4,000 rpm for 10 min. Protein concentrations of fraction was estimated by the Bradford method. The prepared samples were then resolved on a 10% SDS-PAGE. Electrophoresed proteins were transferred to PVDF membranes and blocked for 2 hours at ambient temperature in tris-buffered saline containing 5% (w/v) bovine serum albumin (BSA). After blocking, membranes where incubated overnight at 4°C with primary antibody to

Akt1(1:1000) dilution, followed the next day by 1 hour incubation with secondary antibody labeled with horseradish peroxidase (1:5000) dilution. Immunostained bands were detected by Enhanced Chemiluminescence kit (ECL Amersham Pharmacia Biotech, France).

3.6.1 Estimation of protein

The concentration of the protein was estimated using Bradford method. OD was measured at 595 nm. A standard linear plot of OD vs. BSA concentration (mg/ml) was constructed. Protein content was then determined using the standard graph.

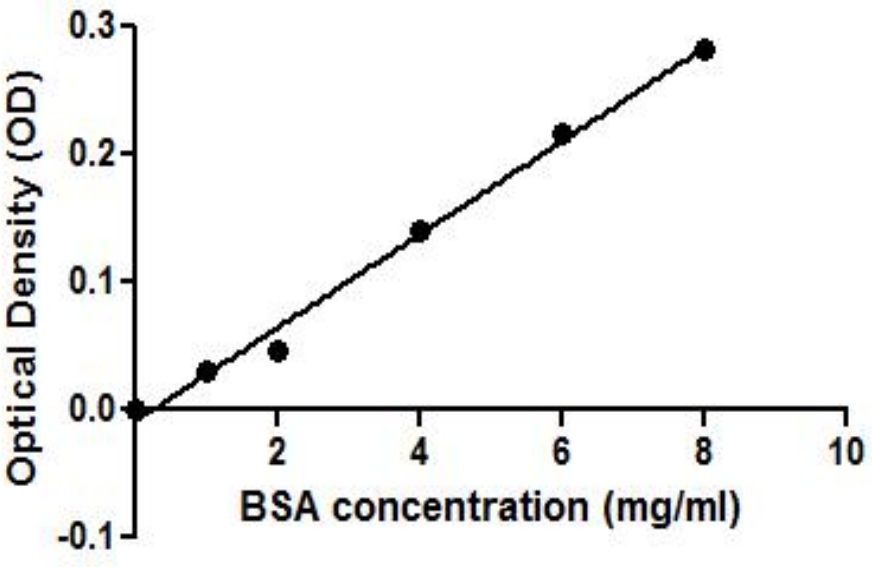

Fig 5: Standard graph to determine protein content

Calculation

$$\text{Protein content (mg/ml)} = \frac{\text{Standard OD} \times \text{Dilution factor} \times \text{Observed OD}}{100}$$

3.6.2 Gel reagents

The prepared samples were resolved on 10% SDS PAGE. The gel reagents used to prepare 10% SDS PAGE are: 1) *Resolving gel* (contained 5.25% acrylamide, 0.27%

bis-acrylamide, 0.037 M Tris pH 8.8 and 8 M Urea). For 10 ml of resolving gel, 67 µl of 10% ammonium persulphate (APS) and 20 µl of TEMED were added. 2) *Stacking gel* (contained 2.5% acrylamide, 0.075% bis-acrylamide, 0.12% Tris pH 6.6 and 8 M Urea). For 5 ml of stacking gel, 34 µl of 10% APS and 10 µl of TEMED were added.

3.7 Statistical analysis

Statistical analysis was carried out using one-way analysis of variance (ANOVA), followed by Tukey's post-test. Statistical significance was accepted at a p value < 0.05. The data are reported as bar diagrams of mean ± SD, where $n = 3$. The transfected and transduced cells were counted using ImageJ software.

4. Results

4.1 Restriction digestion of plentiCamKII plasmid

20 µl of four different restriction digestion reactions were carried out and were kept at 37°C for an hour. The reactions were then run on 1% agarose gel. As a control an uncut plasmid was loaded in the 5th well. 1 Kb DNA ladder was run alongside to mark the DNA length.

By using EcoRI and BamHI restriction enzymes, plentiCamKII backbone was isolated.

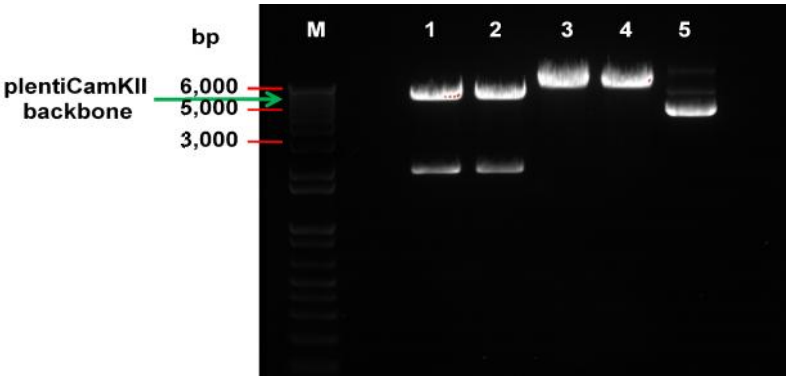

Fig 6: Lane 1, 2 represents double digestion with BamHI and EcoRI, Lane 3 represents single digestion with BamHI, Lane 4 represents single digestion with EcoRI and Lane 5 represents uncut plasmid.

4.2 MyrAkt1 and pmCherry gradient PCR

Gene specific primers were designed for MyrAkt1 and pmCherry. Forward primer BamHI and reverse primer KpnI were designed for MyrAkt1 whereas for pmCherry forward primer KpnI and reverse primer EcoRI were designed and then amplified using gradient PCR which was run at different temperatures (52°C, 55°C, 57°C, 60°C and 62°C). After PCR amplification 10 µl gradient PCR reactions (DNA mix, Buffer, forward primer, reverse primer, DNA template and water) were run on 1% agarose gel. 1 Kb DNA ladder was run alongside to mark the DNA length.

Gene specific primers were amplified using gradient PCR to optimize the conditions before using Phusion PCR. It worked equally well at all the given temperatures.

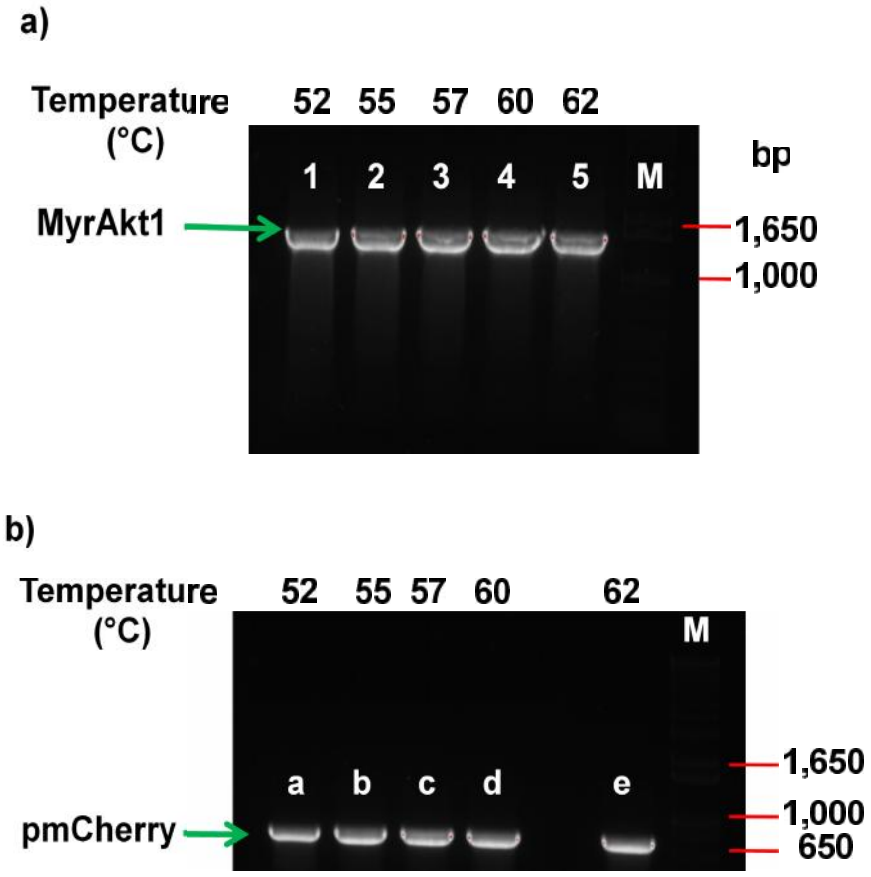

Fig 7: a) Lane 1, 2, 3, 4 and 5 represents band at 1473 bp of BamHI-MyrAkt1-KpnI gradient PCR product; b) Lane a, b, c, d and e represents band at 714 bp of KpnI-pmCherry-EcoRI gradient PCR product.

4.3 MyrAkt1 and pmCherry Phusion PCR

For MyrAkt1 forward primer BamHI and reverse primer KpnI whereas for pmCherry forward primer KpnI and reverse primer EcoRI were designed. The gene with specific primer was then amplified using phusion PCR and was run at temperatures 54°C and 56°C. 10 µl phusion reactions (Buffer, forward primer, reverse primer, DNA template, 10 mM dNTPs, DMSO, phusion, water) was run on 1% agarose gel. To mark the DNA length 1 Kb DNA ladder was loaded.

Gene specific primers worked equally well at 54°C and 56°C, which was then amplified using Phusion PCR (high fidelity DNA polymerase).

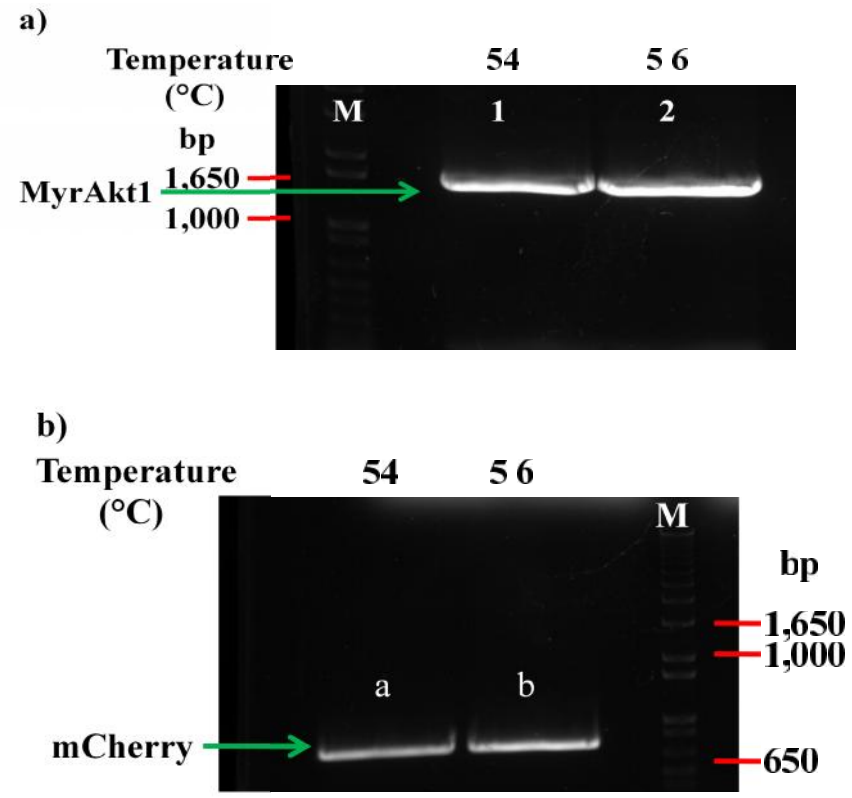

Fig 8: a) Lane 1 and 2 represents band at 1473 bp of BamHI-MyrAkt1-KpnI phusion PCR product; b) Lane 3 and 4 represents band at 714 bp of KpnI-pmCherry-EcoRI Phusion PCR product.

4.4 Cloned MyrAkt1-pmCherry construct confirmed with restriction digestion

Eight reactions (consisting of restriction digestion of amplified fragments) each of 20 µl were incubated for 1 hour at 37°C and then run on 1% agarose gel. First four reactions labeled 1, 2, 3 and 4 consist of 10x fast digestion buffer, transferring plasmid (MyrAkt1-pmCherry construct cloned into plentiCamKII backbone) and restriction enzyme BamHI and KpnI. Next Four reactions labeled a, b, c and d consist of 10x fast digestion buffer, transferring plasmid (MyrAkt1-pmCherry construct cloned into plentiCamKII backbone) and restriction enzyme KpnI and EcoRI. Along with the above eight reactions 1 kb DNA ladder was run to mark the DNA length.

Restriction digestion was performed which confirmed the plasmid by giving out appropriate bands at 1473 bp and 714 bp for MyrAkt1 and pmCherry respectively.

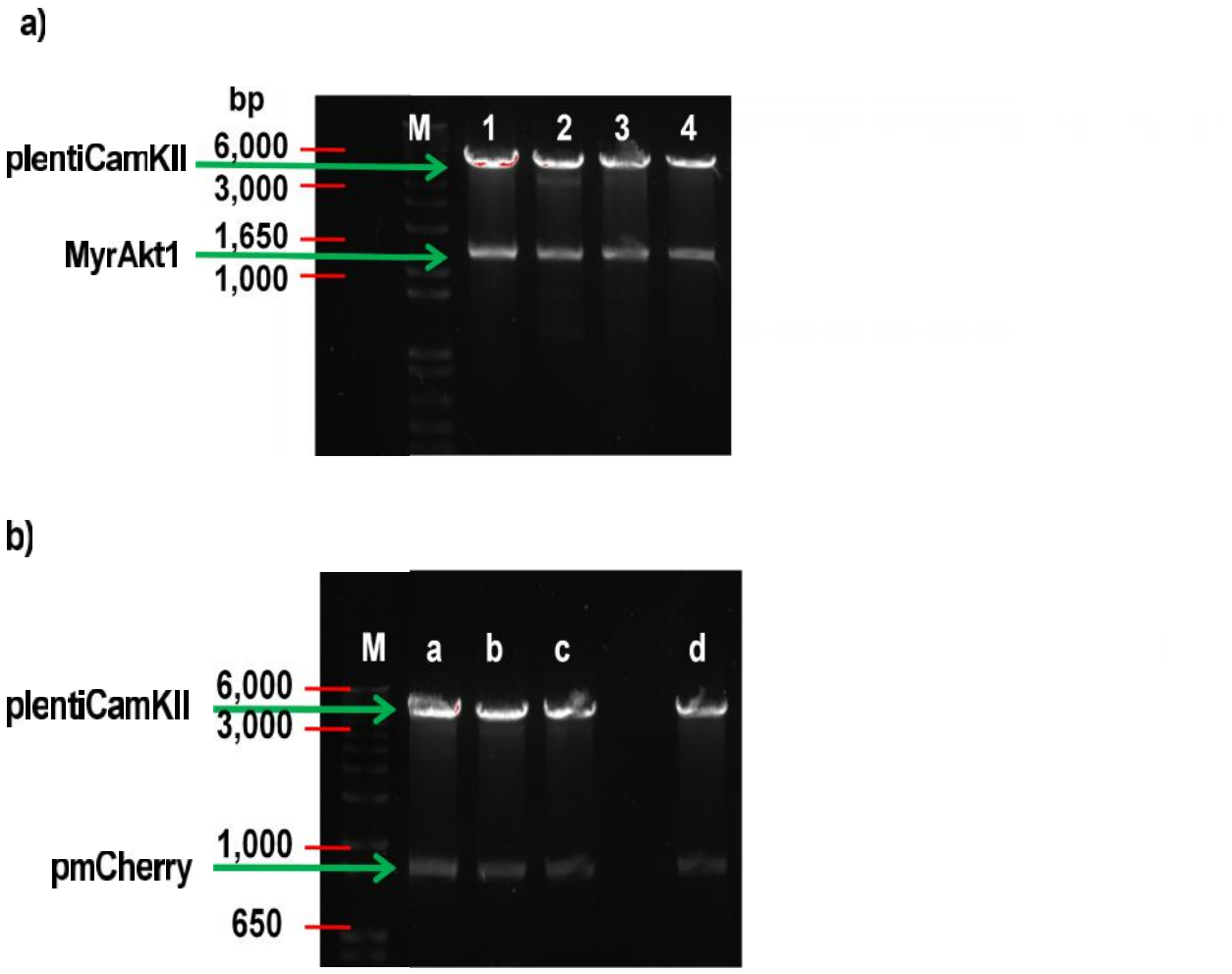

Fig 9: a) Lane 1, 2, 3 and 4 represents the band at 5385 bp of plentiCamKII backbone whereas band at 1473 bp of MyrAkt1 insert; b) Lane a, b, c and d represents the band at 5385 bp of plentiCamKII backbone whereas band at 714 bp of pmCherry tag.

4.5 Expression of MyrAkt1-pmCherry construct confirmed by western blot

To determine the levels of MyrAkt1-pmCherry, HEK293T cells were transfected with MyrAkt1-pmCherry plasmid and the cell lysate was derivatised with anti MyrAkt1 antibody and then the level of MyrAkt1-pmCherry was assayed using western blotting.

Western blot analysis showed an immunoreactive band at the expected molecular weight range in-case of transfected cells but none in-case of untransfected cells confirming the appropriate construction of the cloned plasmid.

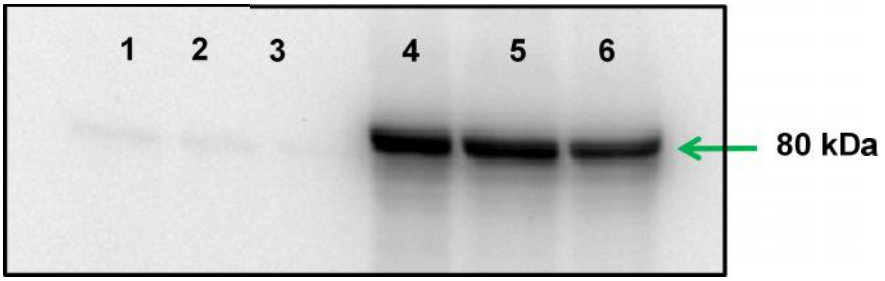

Fig 10: Western blots depicting levels of MyrAkt1-pmCherry. Lane 1, 2 and 3 represents untransfected cells whereas lane 4, 5 and 6 represents transfected cells.

4.6 Sanger analysis for plentiCamKII-MyrAkt1-pmCherry

The transfer vector plasmid (plentiCamKII-MyrAkt1-pmCherry) was sent for Sanger sequencing, with the help of NCBI website the obtained sequencing result were blasted and correctly matched for the known sequence of MyrAkt1-pmcherry.

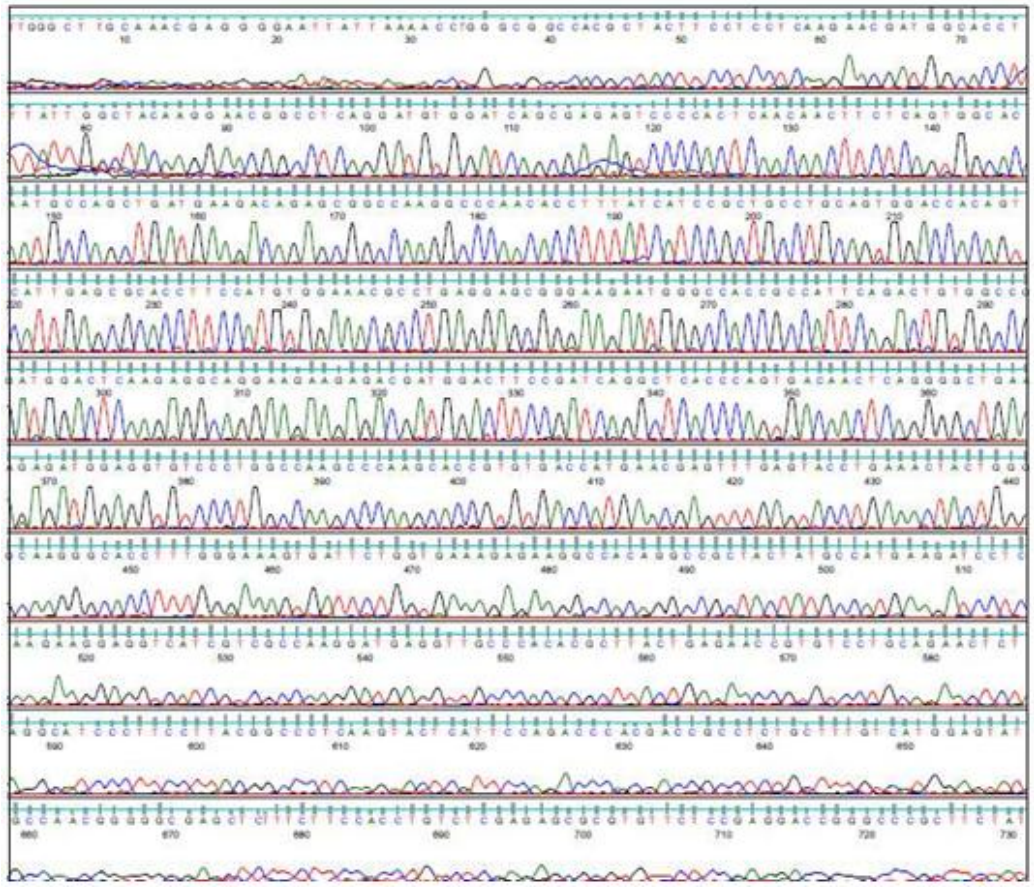

FASTA sequence

TTGGGCTTGCAAACGAGGGGAATTATTAAAACCTGGGCGGCCACGCTACTTCCTCCTCAAGAACG
ATGGCACCTTTATTGGCTACAAGGAACGGCCTCAGGATGTGGATCAGCGAGAGTCCCCACTCAAC
AACTTCTCAGTGGCACAATGCCAGCTGATGAAGACAGAGCGGCCAAGGCCCAACACCTTTATCAT
CCGCTGCCTGCAGTGGACCACAGTCATTGAGCGCACCTTCCATGTGGAAACGCCTGAGGAGCGGG
AAGAATGGGCCACCGCCATTCAGACTGTGGCCGATGGACTCAAGAGGCAGGAAGAAGAGACGATG
GACTTCCGATCAGGCTCACCCAGTGACAACTCAGGGGCTGAAGAGATGGAGGTGTCCCTGGCCAA
GCCCAAGCACCGTGTGACCATGAACGAGTTTGAGTACCTGAAACTACTGGGCAAGGGCACCTTTG
GGAAAGTGATTCTGGTGAAAGAGAAGGCCACAGGCCGCTACTATGCCATGAAGATCCTCAAGAAG
GAGGTCATCGTCGCCAAGGATGAGGTTGCCCACACGCTTACTGAGAACCGTGTCCTGCAGAACTC
TAGGCATCCCTTCCTTACGGCCCTCAAGTACTCATTCCAGACCCACGACCGCCTCTGCTTTGTCA
TGGAGTATGCCAACGGGGGCGAGCTCTTTCTTCCACCTGTCTCGAGAGCGCGTGTTCTCCGAGGA
CCGGGCCCGCTTCTATGGTGCGGAGATTGTGTCTGCCCTGGACTACTTGCACTCCGAGAAGAACG
TGGTGTACCCGGGACCTGAAGCTGGAGAATCCTCATGCTGGACAAGGACGGGCACATCAAGATAA
CGGACTTCGGGCTGTGCAAGGAGGGGATCAAGGA

Fig *11*: Sanger sequencing analysis representing Sanger trace and FASTA sequence for cloned plentiCamKII-MyrAkt1-pmCherry plasmid (transform vector plasmid).

4.7 HEK293FT cells were successfully co-transfected with three separate plasmids

HEK293FT cells were co-transfected using calcium phosphate method with transfer vector plasmid (MyrAkt1-pmCherry construct), packaging plasmid (PsPAX2) and envelop plasmid (pMD2.G).

Transfection efficiency increased with time, 48 hours being the appropriate time needed to observe transfected cells.

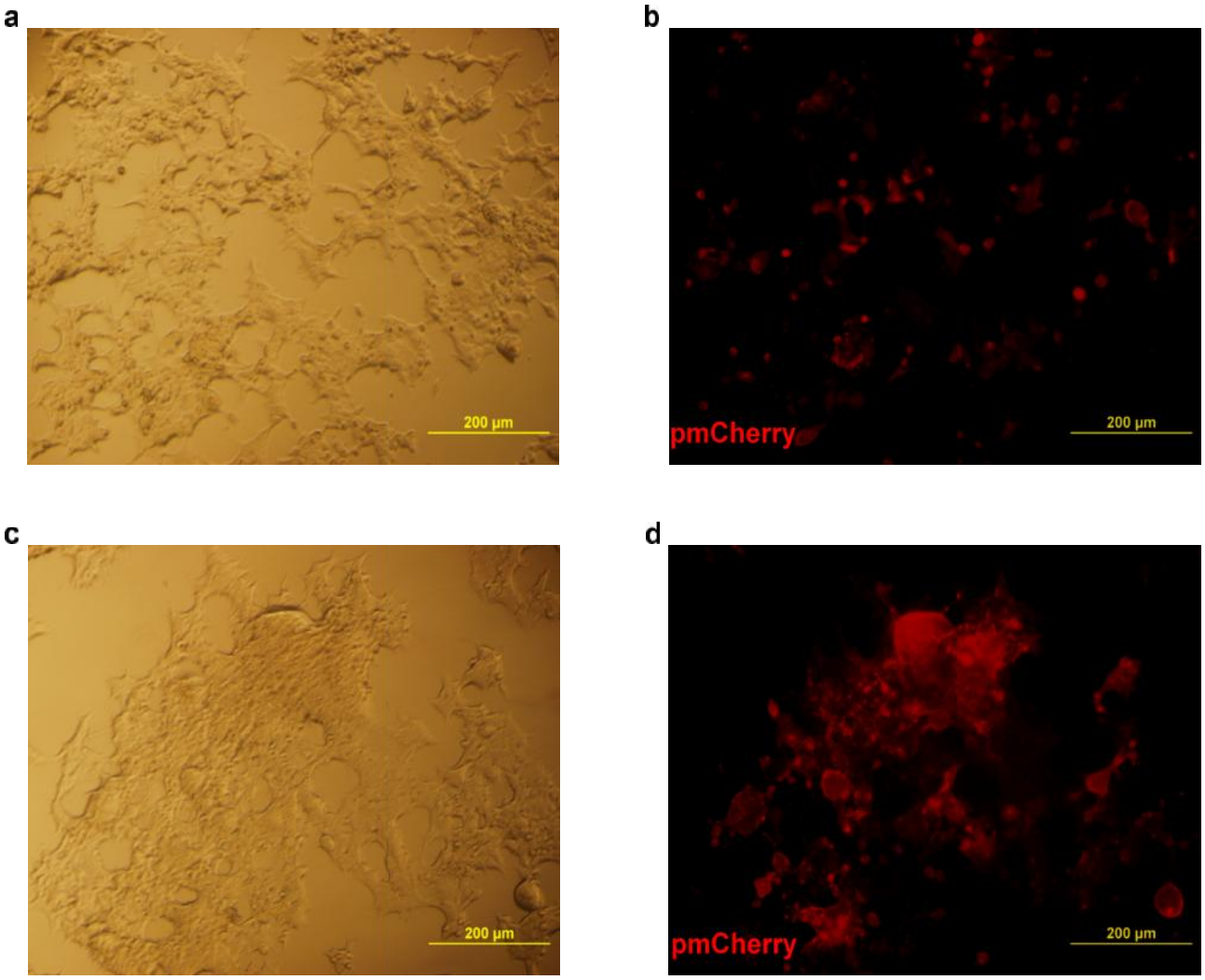

Fig 12: CamKII promoter-driven expression of MryAkt1-pmCherry in HEK293T cells: a) Bright field image of cells infected after 24 hours; b) Fluorescent image of cell infected after 24 hours; c) Bright field image of cells infected after 48 hours; b) Fluorescent image of cell infected after 48 hours.

4.7 Estimated transfection efficiency analysis

~87.5% transfection efficiency was achieved in ~95% confluent 100 mm plate.

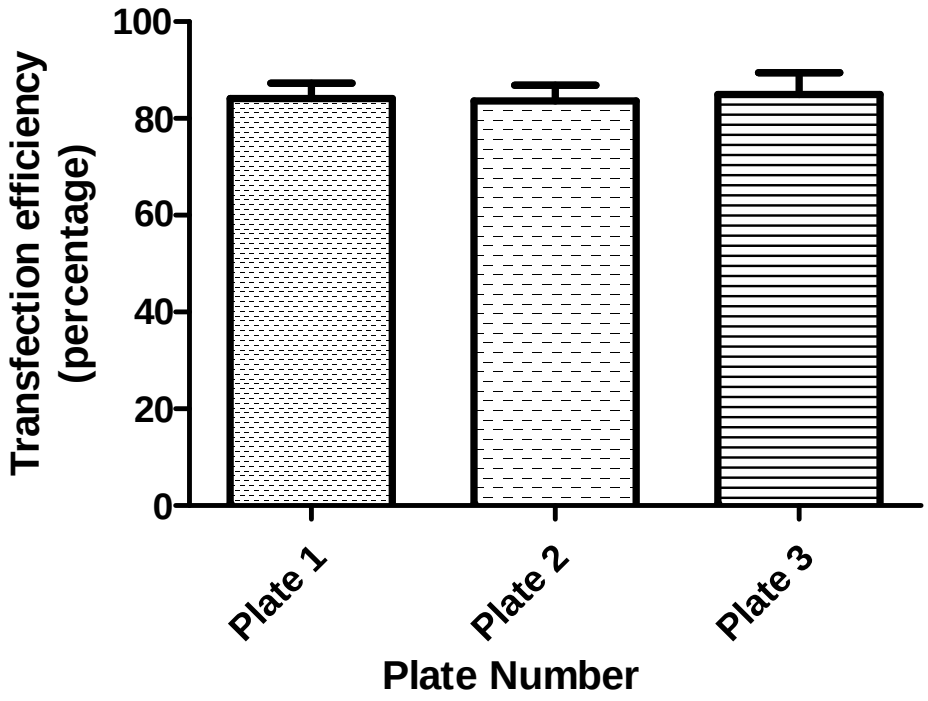

Figure 13: Plot to represent the estimated transfection efficiency. About 48 hours after transfection fluorescent cells were counted using fluorescent microscopy. Each data point represents percentage of transfected cells calculated from three different fields of views in a 100 mm plate. Error bars indicate standard deviation of the mean.

4.8 HEK293T cells were successfully transduced with MyrAkt1-pmCherry construct packaged in a lentivirus with good viability of purified virions.

100 µl of concentrate viral solution was obtained by density gradient ultracentrifugation of filtered media (0.45 µm PVDF-membrane filter) in which HEK293FT cells were grown and transfected. To estimate the virus titer, micro-liter volumes of pre-concentrate was added to wells in a twelve well plate with comparable cell number.

With increasing dose of viral concentration the number of transduced HEK293T cells increased, 30µl of viral concentration being the appropriate dose amount needed for transduction.

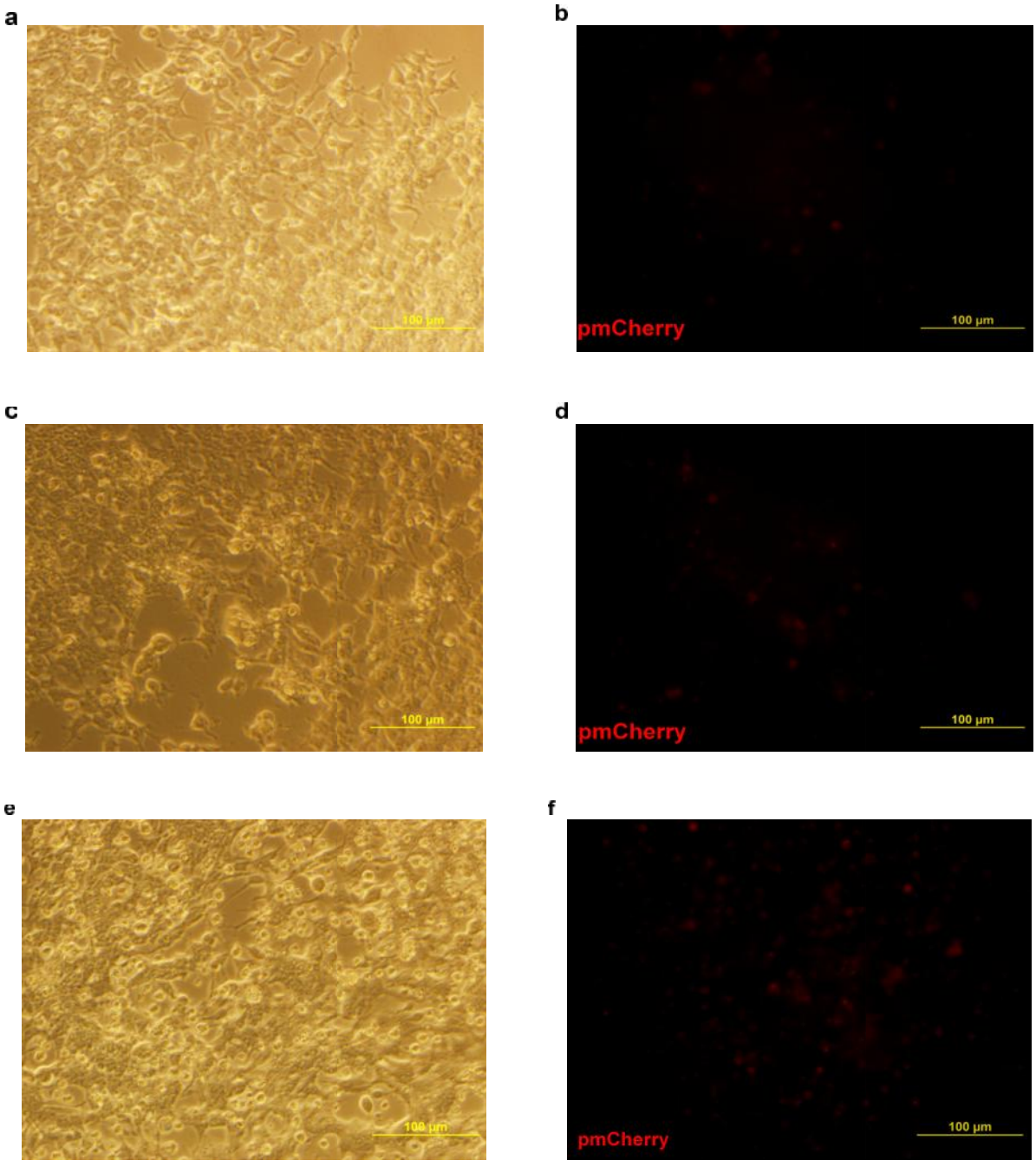

Figure 14: CamKII promoter-driven expression of MryAkt1-pmCherry in HEK293T cells: a) Bright field image of cells infected with 10 µl of lentiviral concentrate; b) Fluorescent image of cells infected with 10 µl of lentiviral concentrate; c) Bright field image of cells infected with 20 µl of lentiviral concentrate; d) Fluorescent image of cells infected with 20 µl of lentiviral concentrate; e) Bright field image of cells infected with 30 µl of lentiviral concentrate; f) Fluorescent image of cells infected with 30 µl of lentiviral concentrate.

4.9 Estimated lentiviral titer was found to be ~10^6 infectious units per ml of lentiviral concentrate

Using 30 µl viral concentrate, ~66% transduction efficiency was achieved in ~100% confluent well. Estimated number of cells in each well was ~1×10^5. R^2 value was found to be 0.95.

Titer value of 2.2×10^6 TU/ml was obtained in 100% confluent 12 well plate.

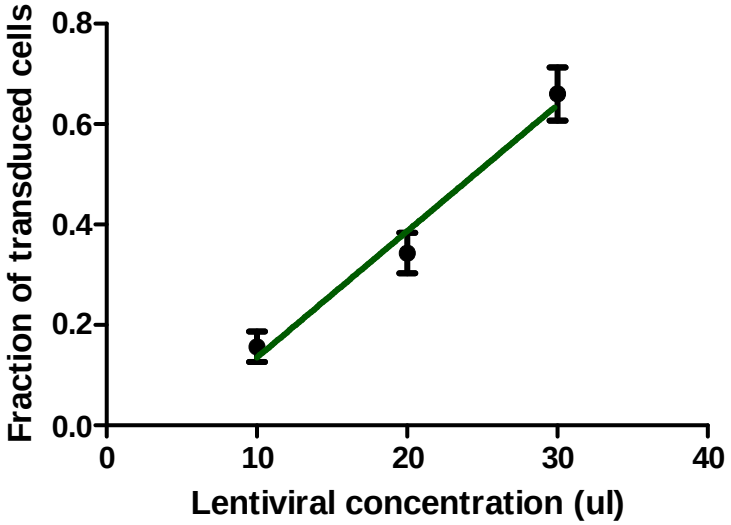

Figure 15: Plot to represent the estimated virus titer. Transduction was performed using 5 mg/ml of hexadimethrine bromide along with concentrated virus solution. Each data point represents mean fraction of transduced cells calculated from three different fields of views in a 12 well plate. Error bars indicate standard deviation of the mean. R^2 value was found to be 0.95.

4.10 Western blot to confirm expression of MyrAkt1-pmCherry after lentivirus production

To determine the levels of MyrAkt1, HEK293T cells were transduced with lentivirus containing MyrAkt1-pmCherry plasmid and the cell lysate was derivatised with anti MyrAkt1 antibody and then the level of MyrAkt1 was assayed using Western blotting.

In the blot, in case of cells transduced with lentivirus containing MyrAkt1-

pmCherry construct two bands were obtained, lower band depicting endogenous Akt1 whereas the upper band at 80 kDa depicting over-expressed myristoylated Akt1 along with pmCherry tag. In the untransduced cells only one band of endogenous Akt1 was observed thus confirming the appropriate lentivirus generation.

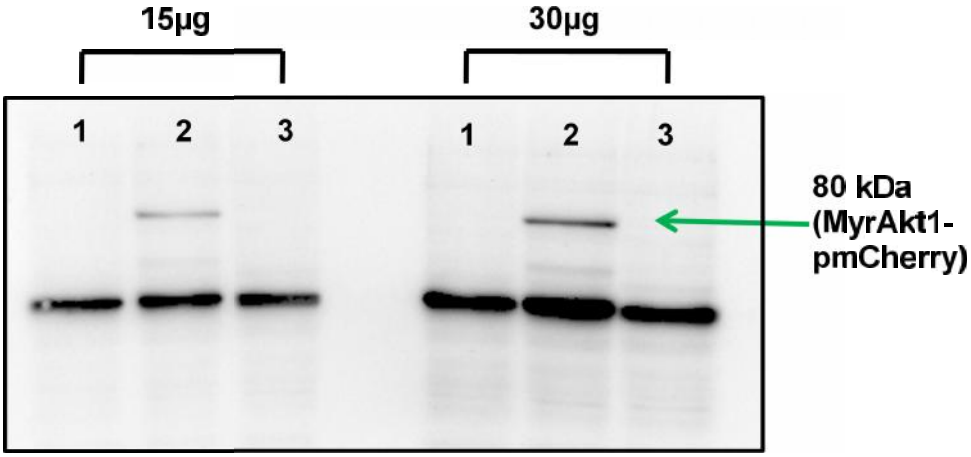

Fig 16: Western blots depicting levels of MyrAkt1. In first three wells protein concentration of 15 µg was loaded whereas in next three wells protein concentration of 30 µg was loaded. Lane 1 represents untransduced cells, lane 2 represents transduced cells with lentivirus containing MyrAkt1-pmCherry plasmid and lane 3 represents transduced cells with lentivirus containing pmCherry plasmid.

4.11 Neuro2A (N2A) cells were transduced with MyrAkt1-pmCherry construct packaged in a lentivirus with good viability of purified virions.

100 µl of concentrate viral solution was obtained by density gradient ultracentrifugation of filtered media (0.45 µm PVDF-membrane filter) in which HEK293T cells were grown and transfected. A micro-liter volume of pre-concentrate was added to wells in a twelve well plate containing N2A cells.

N2A cells were transduced with 30 µl of viral concentration which gave an efficiency of 44.44%.

a) b)

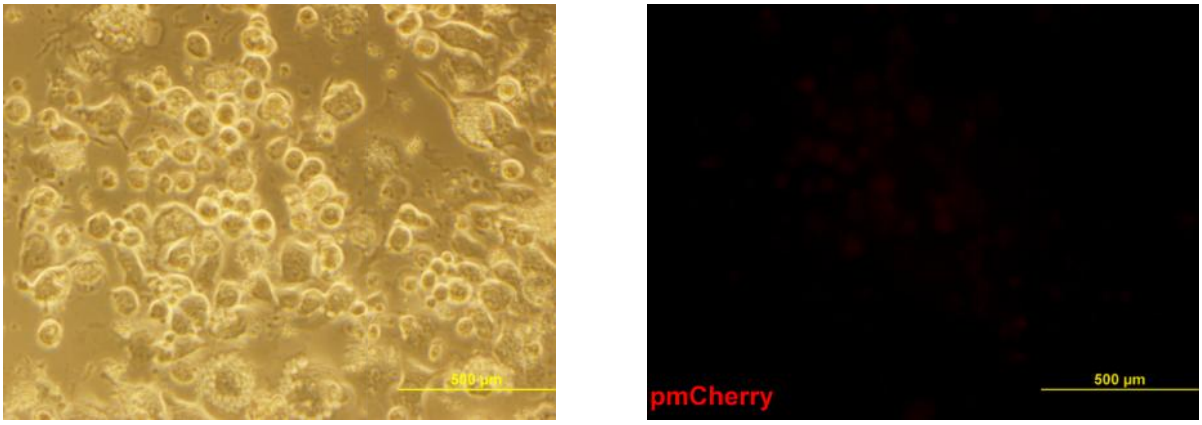

Figure 17: CamKII promoter-driven expression of MryAkt1-pmCherry in N2A cells: a) Bright field image of cells infected with 30 µl of lentiviral concentrate; b) Fluorescent image of cells infected with 30 µl of lentiviral concentrate.

5. Discussion

Synaptic dysfunction and loss of dendritic spines is a cardinal feature observed in the early stage of AD. Previous studies from our lab have shown oxidative stress as one of the mechanism for this dysfunction in AD. Generation of reactive oxygen species (ROS) leads to deregulated activity dependent protein translation at the synapse which in turn leads to changes in synaptic structure and function. Interestingly, studies in our lab have shown a critical role of Akt1 in activity-dependent translation. Also we have observed synapse-specific deregulation of Akt1 signaling very early in our AD mouse model. Hence to test whether disruption of Akt1 is indeed one of the primary contributors to AD pathogenesis we sought to employ over-expression strategies for Akt1 in neuronal cultures obtained from transgenic AD mice. To this front, lentivirus was designed as a gene therapy tool to over-express Akt1 exogenously in the transgenic mice.

Designing three plasmids for second generation lentivirus packaging system was the first step towards lentivirus generation. To begin with transforming plasmid was first cloned. plentiCamKII, MyrAkt1 and pmCherry were selected as backbone, gene of interest and fluorescent tag respectively. Gene specific primers, BamHI (forward primer), KpnI (reverse primer) whereas KpnI (forward primer), EcoRI (reverse primer) were designed for MyrAkt1 and pmCherry respectively. It was then amplified using gradient and phusion PCR and then inserted into the desired plentiCamKII backbone. To confirm the design plasmid different methods were carried out. Initially a restriction digestion was performed which confirmed the plasmid by giving out appropriate bands at 1473 bp and 714 bp for MyrAkt1 and pmCherry respectively. Then the plasmid was sent for Sanger sequencing, with the help of NCBI website the obtained sequencing result were blasted and matched for the known sequence. Western blot analysis showed an immunoreactive band at the expected molecular weight range in-case of transfected cells but none in-case of untransfected cells, further confirming the appropriate construction of the cloned plasmid. Other two plasmids for virus generation (packaging and envelop) were obtained from Dr. Balaji Jayaprakash's lab.

HEK293FT cells were cultured and then transfection on HEK293FT was standardized using calcium phosphate co-transfection method. Transfection efficiency was calculated

by observing cells under fluorescent microscope. 87.5% transfection efficiency was achieved in 95% confluent 100 mm plate. To calculate the titer value of the generated virus it was then transduced in HEK293T cells. Different dilution factors as well as polybrene concentration were tested while standardizing viral transduction on HEK293T cells. Finally a titer value of 2.2×10^6 TU/ml was obtained in 100% confluent 12 well plate. To further confirm that the generated virus indeed contains the desired gene of interest (MyrAkt1), western blotting was employed. In the blot, in case of cells transduced with lentivirus containing MyrAkt1-pmCherry construct two bands were obtained, lower band depicting endogenous Akt1 whereas the upper band at 80 kDa depicting over-expressed myristoylated Akt1 along with pmCherry tag. In the untransduced cells only one band of endogenous Akt1 was observed thus confirming the appropriate lentivirus generation.

To further validate the generation of lentivirus, a different cell line Neuro2A (N2A) was transduced with 30 µl of viral concentration, which gave an efficiency of 44.44%. Rigorous experiments on different cell-line were performed to validate the successful generation of lentivirus.

Since Akt1 is known as a critical survival protein in the cell. Transducing lentiviral construct of MyrAkt into primary neurons from Alzheimer's disease transgenic mice could protect these neurons from the structural changes in spine pathology that occurs due to excessive production of Aβ42. It can play a protective role and restore the spine number, spine density and spine morphology. Thus generation of a transducible virus capable of myristoylated Akt1 to treat dysregulated molecular pathways downstream of Aβ may enable us to manipulate dendritic spine *in vivo* and help in the treatment and prevention of AD.

6. Conclusion

The project is highlighted by successful preparation of a transducible virus optimized for myristoylated Akt1 production. The efficiency of viral transduction was optimized for over expression of myristoylated Akt1 in N2A cells. Since our hypothesis involves an oxidative stress mediated dysfunction of Akt1 signaling as a critical molecular pathway for AD pathogenesis, generation of a transducible virus capable of myristoylated Akt1 is a major breakthrough in research for identifying the molecular mechanisms of AD pathogenesis and devising therapeutic measures against it. This molecular tool will be used both for testing our hypothesis using primary neurons from AD transgenic mice and as an important technique for verifying whether Akt1 overexpression is capable of reversing, at least in part, the structural and functional deregulations observed in synapses of AD mice.

References

Arendt, T. (2009). Synaptic degeneration in Alzheimer's disease. Acta Neuropathol. *118*, 167–179.

Bertram, L., and Tanzi, R.E. (2008). Thirty years of Alzheimer's disease genetics: the implications of systematic meta-analyses. Nat. Rev. Neurosci. *9*, 768–778.

Bertram, L., and Tanzi, R.E. (2011). Genetics of Alzheimer's Disease. In Neurodegeneration: The Molecular Pathology of Dementia and Movement Disorders: Second Edition, (Wiley-Blackwell), pp. 51–61.

Braak, H., and Braak, E. (1991). Neuropathological stageing of Alzheimer-related changes. Acta Neuropathol. *82*, 239–259.

Breckpot, K., Dullaers, M., Bonehill, A., Van Meirvenne, S., Heirman, C., De Greef, C., van der Bruggen, P., and Thielemans, K. (2003). Lentivirally transduced dendritic cells as a tool for cancer immunotherapy. J. Gene Med. *5*, 654–667.

Bukrinsky, M., Sharova, N., and Stevenson, M. (1993). Human immunodeficiency virus type 1 2-LTR circles reside in a nucleoprotein complex which is different from the preintegration complex. J. Virol. *67*, 6863–6865.

Cleary, J.P., Walsh, D.M., Hofmeister, J.J., Shankar, G.M., Kuskowski, M.A., Selkoe, D.J., and Ashe, K.H. (2005). Natural oligomers of the amyloid-beta protein specifically disrupt cognitive function. Nat. Neurosci. *8*, 79–84.

Datta, S.R., Brunet, A., and Greenberg, M.E. (1999). Cellular survival: A play in three akts. Genes Dev. *13*, 2905–2927.

DeKosky, S.T., and Scheff, S.W. (1990). Synapse loss in frontal cortex biopsies in Alzheimer's disease: correlation with cognitive severity. Ann. Neurol. *27*, 457–464.

Dull, T., Zufferey, R., Kelly, M., Mandel, R.J., Nguyen, M., Trono, D., and Naldini, L. (1998). A third-generation lentivirus vector with a conditional packaging system. J. Virol. *72*, 8463–8471.

Griffin, R.J., Moloney, A., Kelliher, M., Johnston, J. a., Ravid, R., Dockery, P., O'Connor, R., and O'Neill, C. (2005). Activation of Akt/PKB, increased phosphorylation of Akt substrates and loss and altered distribution of Akt and PTEN are features of Alzheimer's disease pathology. J. Neurochem. *93*, 105–117.

Hering, H., and Sheng, M. (2001). Dendritic spines: structure, dynamics and regulation. Nat. Rev. Neurosci. *2*, 880–888.

Kanninen, K., Heikkinen, R., Malm, T., Rolova, T., Kuhmonen, S., Leinonen, H., Ylä-Herttuala, S., Tanila, H., Levonen, A.-L., Koistinaho, M., et al. (2009). Intrahippocampal injection of a lentiviral vector expressing Nrf2 improves spatial learning in a mouse model of Alzheimer's disease. Proc. Natl. Acad. Sci. U. S. A. *106*, 16505–16510.

Kohn, A.D., Takeuchi, F., and Roth, R.A. (1996). Akt, a pleckstrin homology domain containing kinase, is activated primarily by phosphorylation. J. Biol. Chem. *271*, 21920–21926.

Komatsuzaki, Y., Hatanaka, Y., Murakami, G., Mukai, H., Hojo, Y., Saito, M., Kimoto, T., and Kawato, S. (2012). Corticosterone induces rapid spinogenesis via synaptic glucocorticoid receptors and kinase networks in hippocampus. PLoS One *7*.

Lewis, P.F., and Emerman, M. (1994). Passage through mitosis is required for oncoretroviruses but not for the human immunodeficiency virus. J. Virol. *68*, 510–516.

Mautino, M.R. (2002). Lentiviral vectors for gene therapy of HIV-1 infection. Curr. Gene Ther. *2*, 23–43.

Mondragón-Rodríguez, S., Perry, G., Zhu, X., Moreira, P.I., Acevedo-Aquino, M.C., and Williams, S. (2013). Phosphorylation of tau protein as the link between oxidative stress,

mitochondrial dysfunction, and connectivity failure: Implications for Alzheimer's disease. Oxid. Med. Cell. Longev.

Naldini, L., Blömer, U., Gallay, P., Ory, D., Mulligan, R., Gage, F.H., Verma, I.M., and Trono, D. (1996). In vivo gene delivery and stable transduction of nondividing cells by a lentiviral vector. Science *272*, 263–267.

Palù, G., Parolin, C., Takeuchi, Y., and Pizzato, M. (2000). Progress with retroviral gene vectors. Rev. Med. Virol. *10*, 185–202.

Penzes, P., and Jones, K.A. (2008). Dendritic spine dynamics--a key role for kalirin-7. Trends Neurosci. *31*, 419–427.

Proctor, D.T., Coulson, E.J., and Dodd, P.R. (2010). Reduction in post-synaptic scaffolding PSD-95 and SAP-102 protein levels in the Alzheimer inferior temporal cortex is correlated with disease pathology. J. Alzheimer's Dis. *21*, 795–811.

Scheff, S.W., and Price, D.A. (2003). Synaptic pathology in Alzheimer's disease: A review of ultrastructural studies. In Neurobiology of Aging, pp. 1029–1046.

Scheff, S.W., Price, D.A., Schmitt, F.A., and Mufson, E.J. (2006). Hippocampal synaptic loss in early Alzheimer's disease and mild cognitive impairment. Neurobiol. Aging *27*, 1372–1384.

Scheid, M.P., and Woodgett, J.R. (2000). Protein kinases: Six degrees of separation? Curr. Biol. *10*.

Song, G., Ouyang, G., and Bao, S. (2005). The activation of Akt/PKB signaling pathway and cell survival. J. Cell. Mol. Med. *9*, 59–71.

Srivareerat, M., Tran, T.T., Alzoubi, K.H., and Alkadhi, K.A. (2009). Chronic psychosocial stress exacerbates impairment of cognition and long-term potentiation in beta-amyloid rat model of Alzheimer's disease. Biol. Psychiatry *65*, 918–926.

Sultana, R., and Butterfield, D.A. (2009). Oxidatively modified, mitochondria-relevant brain proteins in subjects with Alzheimer disease and mild cognitive impairment. J. Bioenerg. Biomembr. *41*, 441–446.

Townsend, M., Shankar, G.M., Mehta, T., Walsh, D.M., and Selkoe, D.J. (2006). Effects of secreted oligomers of amyloid beta-protein on hippocampal synaptic plasticity: a potent role for trimers. J. Physiol. *572*, 477–492.

Tu, S., Okamoto, S.-I., Lipton, S. a, and Xu, H. (2014). Oligomeric Aβ-induced synaptic dysfunction in Alzheimer's disease. 1–12.

Varadarajan, S., Yatin, S., Kanski, J., Jahanshahi, F., and Butterfield, D.A. (1999). Methionine residue 35 is important in amyloid β-peptide-associated free radical oxidative stress. Brain Res. Bull. *50*, 133–141.

William, C.M., Andermann, M.L., Goldey, G.J., Roumis, D.K., Reid, R.C., Shatz, C.J., Albers, M.W., Frosch, M.P., and Hyman, B.T. (2012). Synaptic Plasticity Defect Following Visual Deprivation in Alzheimer's Disease Model Transgenic Mice. J. Neurosci. *32*, 8004–8011.

Zufferey, R., Nagy, D., Mandel, R.J., Naldini, L., and Trono, D. (1997). Multiply attenuated lentiviral vector achieves efficient gene delivery in vivo. Nat. Biotechnol. *15*, 871–875.